JOURNAL OF MATERIALS SCIENCE **36** (2001) 3365–3371

Toward understanding the stress oscillation phenomenon in polymers due to tensile impact loading

J. KARGER-KOCSIS*, O. I. BENEVOLENSKI
Institut für Verbundwerkstoffe GmbH, Universität Kaiserslautern, Pf. 3049, D-67653 Kaiserslautern, Germany
E-mail: karger@ivw.uni-kl.de

E. J. MOSKALA
Eastman Chemical Company Research Laboratories, POBox 1972, Kingsport, TN 37662-5150, USA

Though stress oscillation phenomena can be triggered by static and dynamic tensile loading in amorphous (co)polyesters, they have nothing in common. Static loading-caused stress oscillation appears to be controlled by strain-induced crystallization and related heat release and thus can be observed only in crystallizable polymers. On the other hand, dynamic loading-induced stress oscillation is a more universal phenomenon as related to the natural frequency of the test set-up. The latter was established by determining the natural frequency of the instrumented anvil via fast Fourier transformation using a crystallized poly(ethylene terephthalate) (cPET) specimen failing brittlely. When the instrumented tensile impact response of amorphous PET (aPET) and commercial copolyesters (Eastar® PCTG and A150, respectively) has been filtered by considering the natural frequency of the test configuration, the related fractograms no longer showed stress oscillation. It was concluded that samples undergoing adiabatic-type multiple shear banding and prone to extensive cold-drawing are the best candidates to demonstrate the onset of dynamic stress oscillation. The latter is favored by low entanglement density of copolyesters.

1. Introduction

Stress oscillation (also termed self-oscillation) during static loading-induced neck propagation of amorphous poly(ethylene terephthalate) (aPET) was first reported in the 1950s ([1–2] and references therein). Stress oscillation means that the necking stress is no longer constant under certain conditions but shows periodic fluctuation in time. The oscillation amplitude, well recognizable in the related stress-strain curves, is fairly constant (cf. Fig. 1). The macroscopic appearance of the stress oscillation is a striation pattern in the necked region of the specimen, which is oriented perpendicular to the loading direction (cf. Fig. 2). The understanding from the few relevant papers [1, 3–4] devoted to the static-loading induced stress oscillation can be summarized as follows:

- stress oscillation occurs during cold drawing of amorphous polymers, which are, however, crystallizable (Note that very recently it has been produced also in initially semicrystalline polymers)
- the onset of stress oscillation depends on the elastic energy stored in the specimen. Therefore it starts in a later stage of necking at constant deformation rate or at higher deformation rate when adopting the technique of step-wise increase of the crosshead speed [4]. The dependence on the specimen size

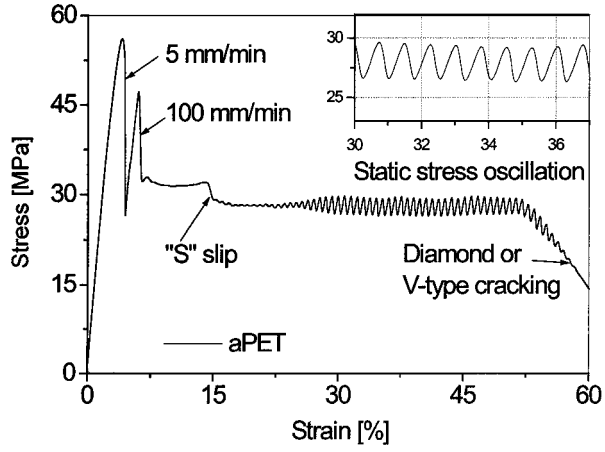

Figure 1 Stress oscillation in the stress-strain curve of an aPET (Eastapak® 9921) dumbbell due to static tensile loading. Testing conditions: stepwise increase of the deformation rate as indicated, room temperature, specimen type: Nr. 3 according to DIN 53455.

* Author to whom all correspondence should be addressed.

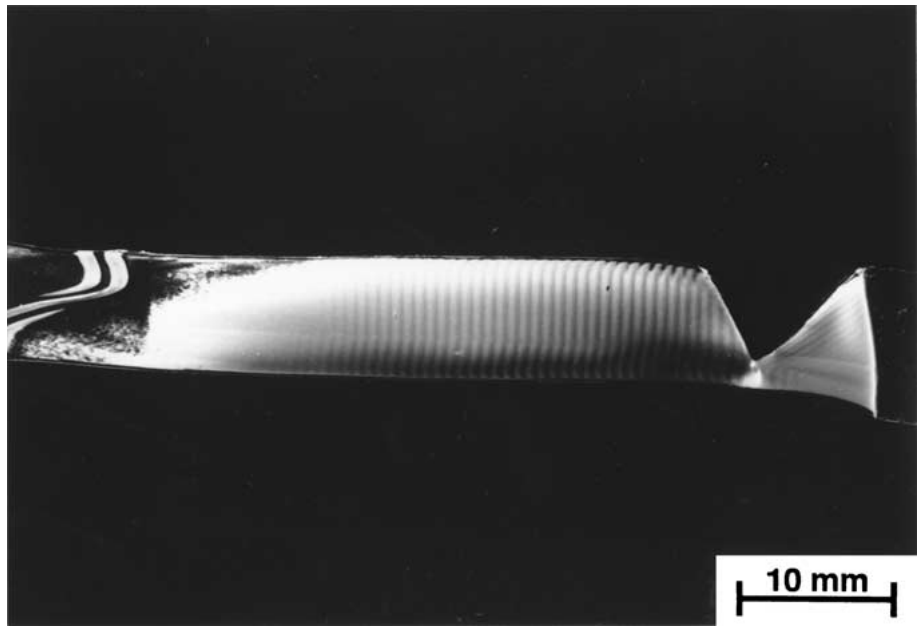

Figure 2 Necked dumbbell specimen showing striation bands due to static stress oscillation. Notes: this specimen was produced in the test shown in Fig. 1. The striations are located between the S slip (left hand side) and V-crack (right hand side).

and configuration can be traced also to changes in the elastic energy stored.

– the rationale behind this stress oscillation phenomenon is a stick-slip mechanism influenced by crystallization. The "stick" stage is due to strain hardening ending up in cold crystallization of the polymer. The "slip" stage is due to the sudden release of the crystallization heat. As a consequence the striation pattern depends also on the testing temperature.

The periodic opaque/transparent striation bands (cf. Fig. 2) are related to crystallized/amorphous PET. Differential scanning calorimetric (DSC) traces corroborate the presence of the banded structure consisting of crystallized and amorphous regions (Fig. 3). Since crystallization is accompanied by volume contraction, voiding should appear if the testing conditions do not allow shrinkage. This is the case under tensile loading, in fact. Fig. 4 shows scanning electron microscopic (SEM) pictures taken through the thickness along the loading direction (Fig. 4a and b). One can see that voiding takes place only in the inner cross-section (Fig. 4a) and the shape of the holes is "discus"-type (cf. Fig. 4b). An alternative explanation for voiding via hydrostatic tension is less likely owing to the small thickness of the polyester sheets used.

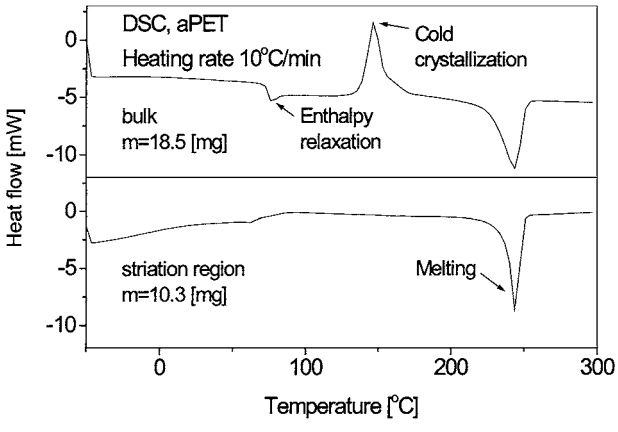

Figure 3 DSC traces taken from the bulk (upper) and striation region (lower) of aPET, respectively.

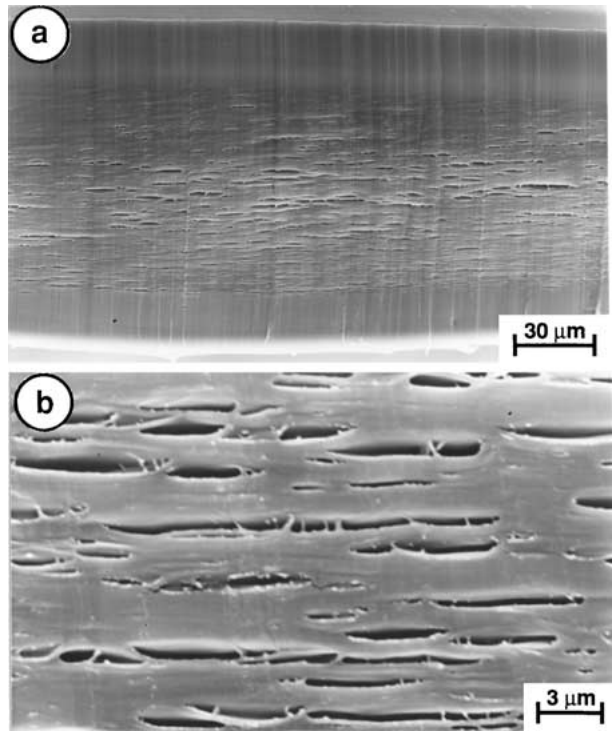

Figure 4 SEM pictures taken on the middle section of the dumbbell (through the thickness) parallel to its loading direction (overview and magnification of the voided area, respectively). Note: voiding is accompanied with thickness increase as demonstrated by picture (a).

Stress oscillation was recently reported to occur also under dynamic tensile loading, i.e. under tensile impact of amorphous copolyesters [5]. The basic difference

between stress oscillation caused by static and dynamic conditions can be summarized as follows [5]:

- stress oscillation is well observed from the beginning of the necking (happening at nearly constant force) and is featured by abating amplitude
- no striation bands and no crystallization can be detected in tensile impacted specimens. Instead of that, shear banding seems to be the dominant deformation mode. The latter is a hint that we are faced with an adiabatic shear banding phenomenon [6, 7]
- the occurrence of stress oscillation is limited to a given impact speed or frequency range.

Other reasons than listed above are also reported to explain recorded oscillations during impact tests. These are inertial loads [8, 9] and harmonic oscillations of the components [8]. These effects are illustrated by simplified dynamic models (using mass and stiffness elements [10]) and models accounting for the vibrations modes of the whole mechanical system [11]. These models, however, impose strong simplification of the material's behavior (assuming linear elastic) or do not implicitly account for non-linearity phenomena. Therefore their application to necking is less straightforward. Another feasible method utilized to handling results of instrumented impact tests is the frequency analysis [10, 12, 13].

Based on the differences in the stress oscillation produced by static and dynamic loading and features of dynamic testing itself, one can presume that their controlling parameters are also different. Focusing on the dynamic oscillation the following questions may be posed:

- are the oscillations recorded during the necking induced by material related mechanism (self-oscillation) or caused by dynamic test conditions. If latter then the stress oscillation should also appear in semicrystalline polymers. This suspicion seems to be supported by some literature reports [14–15].
- which is the deformation mode that favors the stress oscillation during the necking? Further what kind of material parameter may be responsible for it? Information on these issues would help us to understand why stress oscillation was observed only in a given impact speed range of amorphous copolyesters.

The aim of this study was to answer the above questions. Our strategy was to use two kinds of polymers in this work. An aPET, which undergoes stress oscillation during static loading (cf. Fig. 1) and two amorphous copolyesters, which show stress oscillation only under dynamic conditions. If our hypothesis holds, viz. oscillation under tensile impact depends on the test set-up, then we should be able to trigger stress oscillation with both amorphous and semicrystalline PETs under certain dynamic conditions. Studying the failure mode of the copolyesters undergoing stress oscillation only under dynamic conditions, useful information is expected in respect with the favored deformation scenario.

2. Experimental

2.1. Materials

aPET (Eastapak® 9921) and two copolyesters (Eastar® PCTG 5445 denoted as PCTG and Eastar® A150 denoted herein as A150) were supplied in form of thin sheets (thickness about 0.5 mm) by Eastman Chemical Company (Kingsport, TN, USA). The bottle-grade aPET is a copolyester, which contains a small amount of 1,4-cyclohexane dimethylene glycol (CHDM) in order to inhibit crystallization. Nevertheless it was termed aPET throughout this paper. The PCTG also contained (apart of the usual ethylene glycol and terephthalic acid) CHDM precursor in >60 mole %. The glycol component of the A150 is CHDM, whereas the diacid component is a mixture of iso- and terephthalic acids. The inherent viscosity (IV) of the copolyesters was determined in a 0.5 g/100 ml solution of a 60/40 phenol/tetrachloroethane mixture at 25°C and the related values were 0.73, 0.68, and 0.68 dl/g for aPET, PCTG and A150, respectively. aPET and A150 crystallize easily above their glass transition temperature (T_g; cold crystallization), whereas PCTG does so to a lesser extent and closer to the melting range. In order to demonstrate that stress oscillation is likely a common feature for many polymers, a biaxial oriented, filled crystalline PET (BOPET), delivered by ICI Plc., (Wilton, UK) was also used in this study. The thickness of this BOPET film was 0.25 mm.

2.2. Tensile impact tests

Tailed dumbbell specimens (Type A) made according to DIN 53448 were punched from the films and subjected to instrumented tensile impact at room temperature. Tensile impact loading was performed on an instrumented pendulum (Ceast, Pianezza, Italy) at various impact speeds ($v = 1.2$ to 3.7 m/s). This instrumented pendulum allowed us to monitor and store the fracture history of the specimens. The clamping length was kept constant (30 mm).

2.3. Fractography

Cut sections of the broken specimens were inspected by polarized light and scanning electron microscopy (SEM) using a Leitz Diaplan microscope (Wetzlar, Germany) and a Jeol 5400 SEM (Tokyo, Japan). To avoid surface charging the specimens for SEM were sputtered with a gold alloy prior to inspection. These investigations were aimed at elucidating the failure mechanisms.

3. Results and discussions

3.1. Effect of test set-up

During tensile impact the specimen and the anvil oscillate at their natural frequencies, which are detected by the instrumentation of the impact device. Therefore it

is of paramount importance to distinguish between the true mechanical loading and the superimposed stress oscillations and find the frequency of the latter (also called "ringing") [8, 12 and references therein]. This can be done by impacting strong specimens, which fracture in a brittle way. After fracture the clamping rig (anvil) with the built-in sensor continues to oscillate at its natural frequency. The natural frequency can be determined by fast Fourier transformation (FFT) of the ringing [8]. In order to approximate the performance of the material tested in this study, cold crystallized (by keeping the specimen at 140°C for 60 min. in an oven) aPET specimens (cPET) were used as brittle specimens. The cPET specimens failed in a brittle fashion (cf. Fig. 5) [12]. The oscillations for an interval of 5 ms after fracture were subjected to FFT in order to determine the frequency spectrum of the rig (cf. Fig. 5). Fig. 5 also shows the outcome of the FFT analysis. One can see that the highest oscillation amplitude is at about 1.2 kHz what can be treated as the natural frequency of the anvil. Note that this value is very close to the test frequency when it is estimated as the reciprocal value of the time needed to fracture the specimens.

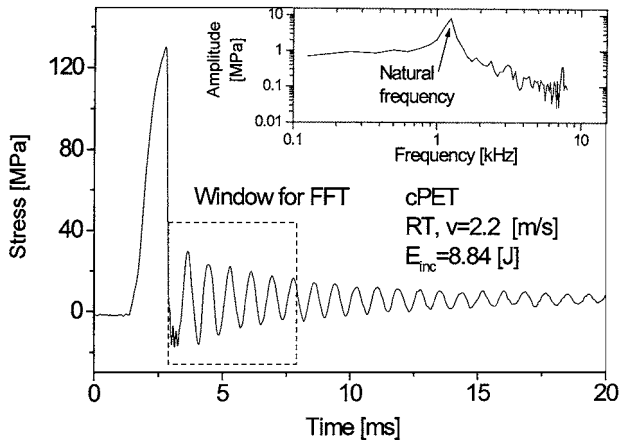

Figure 5 Characteristic stress-time trace of a cPET specimen showing brittle fracture with its frequency spectrum at the ringing. Note: ringing window taken for the FFT analysis is indicated.

3.2. Stress oscillation under dynamic conditions

The amorphous copolyesters PCTG and A150 showed stress oscillation in a rather broad impact speed range. Recall that stress oscillation in these copolyesters could not be produced under static loading. Fig. 6 demonstrates that the oscillation amplitude becomes smaller and its range longer with decreasing impact speed on the example of A150. The results achieved on PCTG samples were similar to those reported in our earlier work [5] except that stress oscillation could be resolved even at the highest available impact speed (i.e. $v = 3.7$ m/s). This finding suggests that the onset of stress oscillation may also depend on the degree of physical aging of the copolyester.

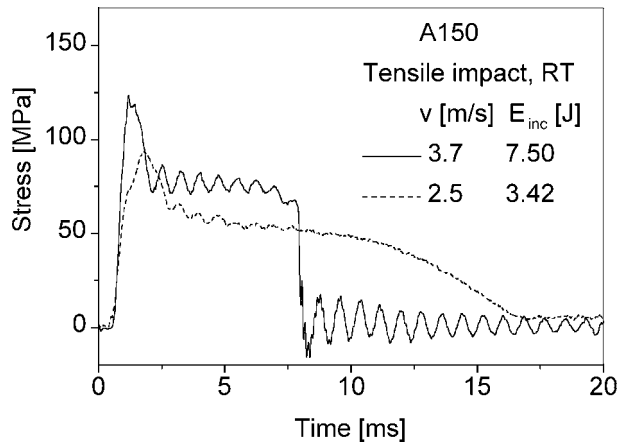

Figure 6 Characteristic stress-time traces of A150 at $v = 3.7$ m/s and $= 2.5$ m/s, respectively.

The scenario was completely different for aPET showing stress oscillation only in a very limited impact speed range (at about 2 m/s). Nevertheless, we succeeded in showing that aPET, prone for stress oscillation under static conditions (cf. Fig. 1), can show this phenomenon also under dynamic conditions. It is worth noting that the stress oscillation in aPET, even in the selected loading range, was less reproducible. This may be related to physical aging of the aPET (see the enthalpy relaxation in the T_g range of the bulk aPET in Fig. 3) and the usual instability of the adiabatic shear bands [7, 16] - see later.

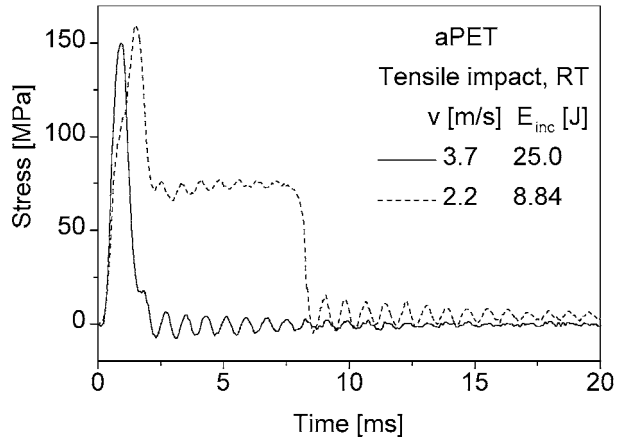

Figure 7 Characteristic stress-time traces of aPET at $v = 3.7$ m/s and $v = 2.2$ m/s, respectively. Note: the maximum energy of the hammer used was 25 J.

3.3. Source of stress oscillation

Looking at the stress-time curves in Figs 5–7 one can get the impression that the oscillation frequency during necking and after fracture of the specimens is practically the same. This suggests that stress oscillation under tensile impact is an artifact triggered by the natural frequency of the test set-up. If this is so, then filtering out the natural frequency from the force (stress)-time curves should result in a smooth curve, which does not show any sign of the recorded oscillation. This is in fact the case, as Fig. 8 displays. Accordingly, stress oscillation under dynamic conditions reflects the effect of the natural frequency of the test setup. So stress oscillation under dynamic conditions should be a quite frequent phenomenon provided that the deformation mode of the polymer specimens favors the necessary necking of the specimen. Next we shall try to point out what

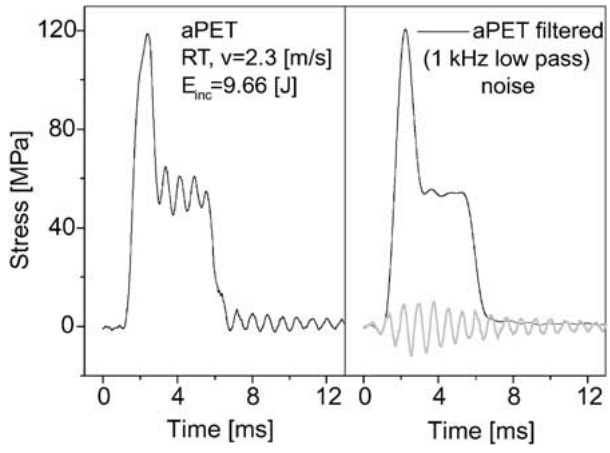

Figure 8 Deconvolution of the experimental stress-time curve of aPET by considering the natural frequency of the anvil. Designation: left—observed curve, right—true mechanical loading. Note: the testing conditions were as follows: *RT*, $v = 2.3$ m/s, $E_{\text{inc}} = 9.66$ J.

are the basic failure mechanisms and which molecular parameters influence them.

3.4. Deformation mechanisms favoring stress oscillation and their molecular relation

It has been shown in our earlier communication that amorphous copolyesters fail under tensile impact by multiple (diffuse) shear banding [5]. Shear banding in amorphous copolyesters is strongly favored if the mean molecular weight between entanglements (M_e) is high, or the entanglement density (v_e) is low [5, 17]. Note that PCTG and A150 possess high M_e (and thus low v_e) values compared to aPET [18]. Consequently, the deformation mode is predominantly multiple or diffuse shear banding. This was found also for specimens of aPET, which failed after showing stress oscillation during tensile impact (Fig. 9). Multiple shear banding increases the overall ductility of the specimen and thus contributes to the appearance of necking. Chen *et al.* [19, 20] and Liu and Yee [21] reported that yielding and necking of amorphous copolyesters and polyestercarbonates containing CHDM units are strongly favored as cyclohexylene rings reduce the barrier between the macromolecular chains and facilitate their slippage.

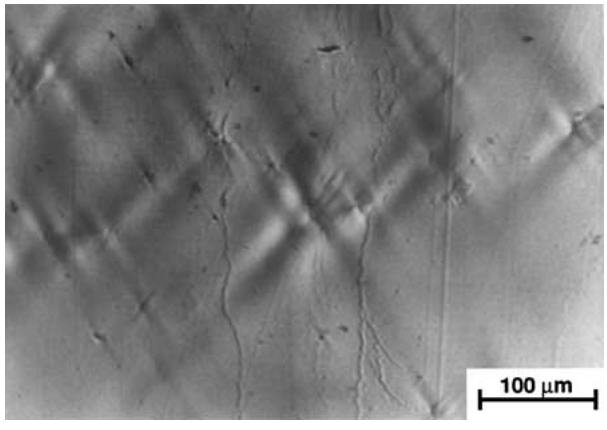

Figure 9 Polarized light microphotograph taken on the necked area of a broken aPET specimen. Note: the intersecting shear bands generate an overall ductile-type deformation ("shear yielding").

They supposed that the related conformational transition ("chair to boat" with a relaxation peak at about −70°C) might be responsible for the toughness increment with increasing CHDM content. During necking the effect of the natural frequency of the test configuration becomes well detectable. Further, shear banding is likely occurring under adiabatic conditions at high speed tensile impact. Though this presumption is intuitive, two supporting facts may be mentioned. First, the failure mode of specimens, which underwent adiabatic shear banding in high-speed compression tests [6] is identical to what we have observed ([5] and cf. Fig. 9). Second, specimens when impacted in tension with various incident impact energies (E_{inc}) but at the same v (such as by changing the mass of the hammer) should show different responses. The experimental results proved this expectation showing that at higher E_{inc} but same v the necking range is less stable. This difference is believed to reflect the fact that adiabatic conditions may be matched in a broader range when impacting the specimens with a hammer of higher kinetic energy. This should influence the formation and coalescence of the shear bands and thus the shape of the tensile impact traces. The importance of spacing of the adiabatic shear bands seems to be in close analogy with the behavior of metals subjected to high strain rates [16].

Analyzing the effect of impact speed and incident impact energy on the total work of fracture of the specimens (cf. Fig. 10) one finds a small scatter for the range $v = 2.5$–3.7 m/s. On the other hand, at lower impact

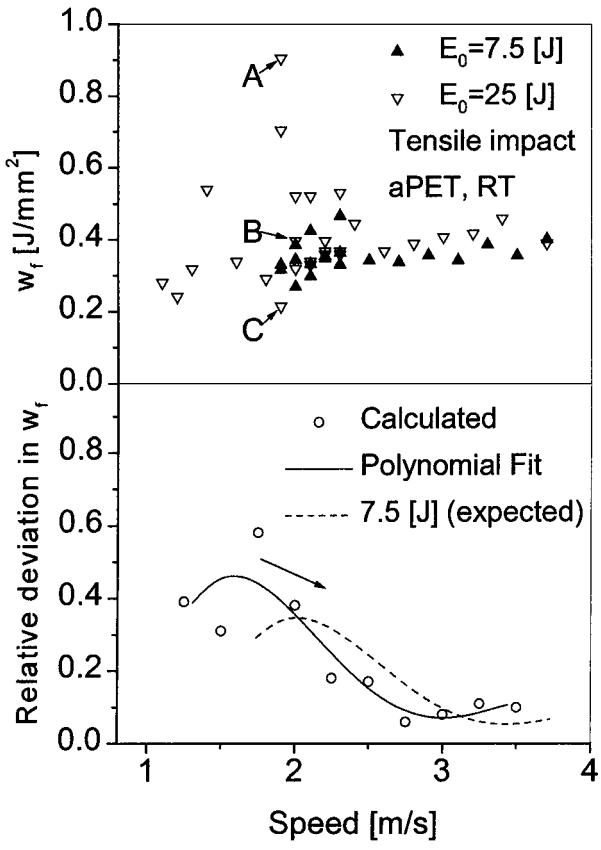

Figure 10 Effect of testing speed and incident impact energy on the total work of fracture (W_f, upper picture) and on its relative deviation (lower picture). Note: as E_{inc} changing with v, the maximum kinetic energy of the hammer at $v = 3.7$ m/s is indicated (7.5 or 25 J).

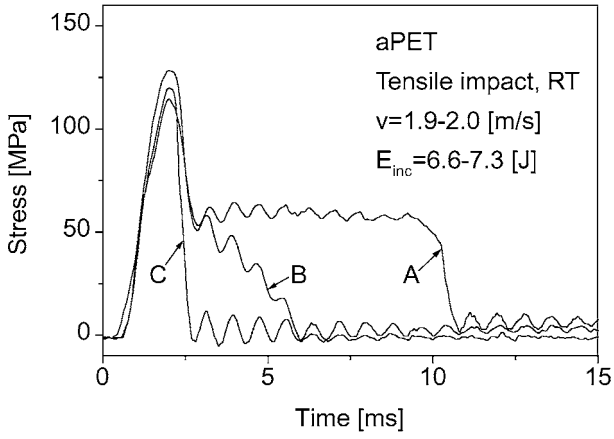

Figure 11 Impact response of characteristic specimens (A, B and C from Fig. 10) showing a large scatter in the total work of fracture.

speeds the scatter rises significantly (cf. Fig. 10). This suggests some uncertainty in the deformation mode.

To estimate the change in the data reliability with decreasing v, the following method has been applied. For each discrete speed value (v_i) starting from 1.25 m/s with a step of 0.25 m/s the standard deviation of the work of fracture was calculated for each sample in the interval $[v_{i-1}, v_{i+1})$ including v_{i-1} and excluding v_{i+1}. Relative deviation was computed with respect to the mean value determined for the same interval. The resulting distribution function shows a maximum at impact speeds in the range 1.5–2.0 m/s.

The effect of incident impact energy is twofold. Firstly, the work of fracture slightly rose with increasing incident energy. This was accompanied by a growing uncertainty in the deformation. Secondly, the maximum of the relative deviation shifted towards smaller impact speeds. The latter fact suggests that the failure uncertainty occurs at a given local strain rate.

In order to study the uncertainty in the deformation mode the specimens A, B and C (as indicted in Fig. 10), were inspected. The stress-time fractograms in Fig. 11 demonstrate that the scatter is due to a premature or even missing necking range. Inspecting the related broken specimens one can trace the reason for the deformation uncertainity (cf. Fig. 12). No necking takes place when the specimen fails along a dominant shear band (specimen C). On the other hand, diffuse shear banding favors the neck formation (specimen A). The result of the latter is a "quasiplastic" deformation ("shear yielding"). The failure mode of the specimen B is between those of A and C (cf. Fig. 12).

The onset of shear banding and shear yielding occurs under adiabatic conditions. It is highly probable that the large scatter in the failure mode is also influenced by surface defects caused by cutting the specimens.

Adiabatic shear banding may take place, however, also in semicrystalline polymers and related composites due to tensile impact. For that purpose polymers with limited yielding and plastic deformation are likely the best model materials. Our selection for BOPET is supported by the fact that its plastic deformation is strongly hampered by the biaxial [22] orientation. In addition, the heat setting procedure applied resulted in a crystalline PET version. Fig. 13 demonstrates a characteristic fractogram of a specimen of filled BOPET. One can clearly see the stress oscillation occurs, however, without considerable yielding (compare Fig. 13 with Figs 7, 8 and 11). It is supposed that the deformation and failure mode in this BOPET is not merely multiple shear banding but it is accompanied also by some voiding. For the onset of the latter, fillers particle acting as stress concentrators may be responsible. Unfortunately, the opacity of the BOPET specimens did not allow us to determine the failure mode exactly. Nevertheless, the fact that BOPET underwent stress oscillation during tensile impact supports our previous claim that this phenomenon is a more general one under dynamic conditions.

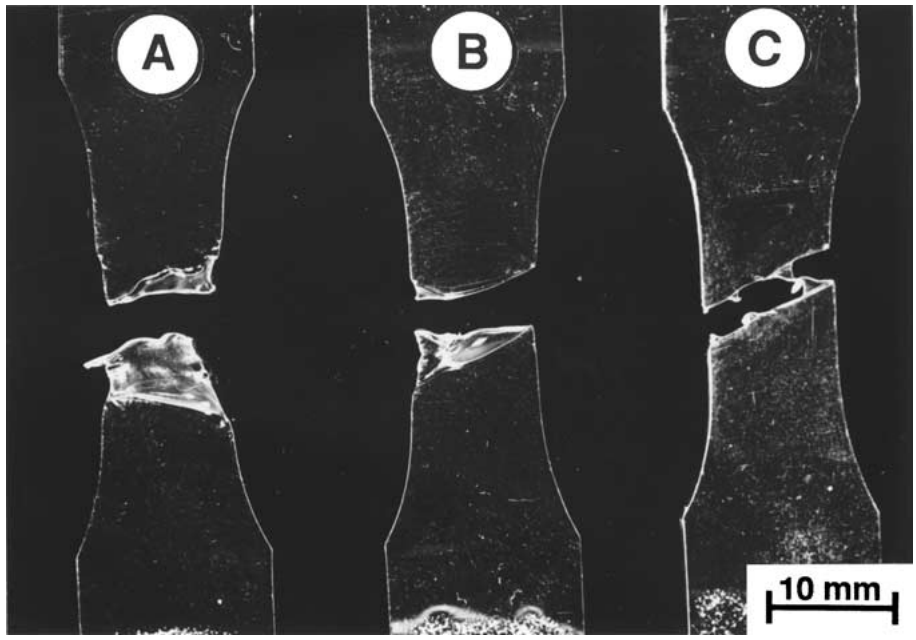

Figure 12 Difference in the fracture mode of the specimens A, B and C. Note: the fractograms of these specimens are depicted in Fig. 11.

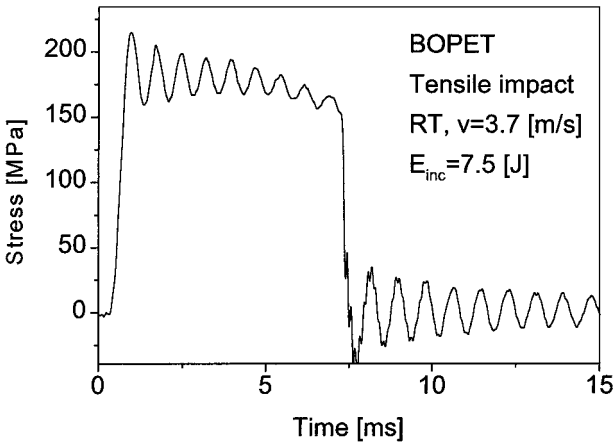

Figure 13 Stress-time traces of a BOPET specimen when impacted under standardized conditions ($v = 3.7$ m/s).

4. Conclusions

The conclusions of this study devoted to the stress oscillation phenomenon caused by tensile impact in amorphous and semicrystalline (co)polyesters can be summarized as follows:

- The stress oscillation is due to the natural frequency of the test set-up. As a consequence, stress oscillation due to dynamic tensile impact is an experiment-related artifact that may appear in many amorphous and semicrystalline polymers. Further, features of the stress oscillation under static and dynamic conditions are completely different. Static stress oscillation appears to be governed by strain-induced crystallization and related heat release and thus observable only in crystallizable polymers. None of the above mentioned preconditions is necessary to produce stress oscillation under tensile impact loading.
- The dominant deformation mechanism associated with dynamic stress oscillation is multiple (diffuse) shear banding under adiabatic conditions. Multiple shear banding is most likely controlled by the entanglement density in amorphous polymers. By contrast, the inherent parameters, which control the onset of stress oscillation in semicrystalline polymers and related systems, are not yet established.

Acknowledgements

The authors are thankful to the Eastman Chemical Co. for the release of this paper. Part of this work was done under a project founded by the German Science Foundation (DFG). Thanks are also due to V. Kordzikau who performed many of the presented tests.

References

1. Y. K. GODOVSKY, "Thermophysical Properties of Polymers" (Springer, Berlin, 1992) p. 221–225.
2. M. C. BOYCE and R. N. HAWARD, in "The Physics of Glassy Polymers," edited by R. N. Haward and R. J. Young, 2nd ed. (Chapman and Hall, London, 1997) p. 251–253.
3. G. P. ANDRIANOVA, A. S. KECHEKYAN and V. A. KARGIN, *J. Polym. Sci. Part A-2* **9** (1971) 1919.
4. H. EBENER, B. PLEUGER and J. PETERMANN, *J. Appl. Polym. Sci.* **71** (1999) 813.
5. J. KARGER-KOCSIS, T. CZIGÁNY and E. J. MOSKALA, *Polym. Eng. Sci.* **39** (1999) 1404.
6. S. M. WALLEY, D. XING and J. E. FIELD, in "Impact and Dynamic Fracture of Polymers and Composites," edited by J. G. Williams and A. Pavan (Mechanical Engineering Publications, London, 1995) p. 289–303.
7. N. A. FLECK, in "Mechanical Properties and Testing of Polymers: An A-Z Reference," edited by G. M. Swallowe (Kluwer Academic, Dordrecht, 1999) p. 15–19.
8. M. C. CHERESH and S. MCMICHEL, in "Instrumented Impact Testing of Plastics and Composite Materials—ASTM STP 936," edited by S. L. Kessler, G. C. Adams, S. B. Driscoll and D. R. Ireland (Am. Soc. Test. Mater., Philadelphia, 1987) p. 9–23.
9. S. SAHRAOUI and J. L. LATAILLADE, *Engng Fract. Mech.* **60** (1998) 437.
10. P. J. CAIN, in "Instrumented Impact Testing of Plastics and Composite Materials—ASTM STP 936," edited by S. L. Kessler, G. C. Adams, S. B. Driscoll and D. R. Ireland (Am. Soc. Test. Mater., Philadelphia, 1987) p. 81–102.
11. S. SAHRAOUI and J. L. LATAILLADE, *Engng Fract. Mech.* **36** (1990) 1013.
12. O. I. BENEVOLENSKI, J. KARGER-KOCSIS, K.-P. MIECK and T. REUßMANN, *J. Thermoplast. Comp. Mater.* **13** (2000) 481.
13. A. I. TOROPOV and M. GROSSO, *J. Test. Eval.* **26** (1998) 315.
14. D. E. MOUZAKIS and J. KARGER-KOCSIS, *J. Appl. Polym. Sci.* **68** (1998) 561.
15. J. KARGER-KOCSIS and J. VARGA, *ibid.* **62** (1996) 291.
16. A. MOLINARI, *J. Mech. Phys. Solids* **45** (1997) 1551.
17. J. KARGER-KOCSIS, in "Handbook of Thermoplastic Polyesters," edited by S. Fakirov (Wiley-VCH, Weinheim, 2001) in press.
18. J. KARGER-KOCSIS, E. J. MOSKALA and P. P. SHANG, *J. Thermal Anal. Calorim.* **63** (2001) 671.
19. L. P. CHEN, A. F. YEE, J. M. GOETZ and J. SCHAEFER, *Macromolecules* **31** (1998) 5371.
20. L. P. CHEN, A. F. YEE and E. J. MOSKALA, *ibid.* **32** (1999) 5944.
21. J. LIU and A. F. YEE, *ibid.* **31** (1998) 7865.
22. J. KARGER-KOCSIS and T. CZIGÁNY, *Polymer* **37** (1996) 2433.

Received 21 July 2000
and accepted 15 February 2001